# G9a selectively represses a class of late-replicating genes at the nuclear periphery

Tomoki Yokochi[a,1], Kristina Poduch[a], Tyrone Ryba[a], Junjie Lu[a], Ichiro Hiratani[a], Makoto Tachibana[b], Yoichi Shinkai[b], and David M. Gilbert[a,2]

[a]Department of Biological Science, Florida State University, Tallahassee, FL 32306; and [b]Experimental Research Center for Infectious Diseases, Institute for Virus Research, Kyoto University, Kyoto 606-8507, Japan

Edited by Mark T. Groudine, Fred Hutchinson Cancer Research Center, Seattle, WA, and approved September 25, 2009 (received for review June 4, 2009)

**We have investigated the role of the histone methyltransferase G9a in the establishment of silent nuclear compartments. Following conditional knockout of the G9a methyltransferase in mouse ESCs, 167 genes were significantly up-regulated, and no genes were strongly down-regulated. A partially overlapping set of 119 genes were up-regulated after differentiation of G9a-depleted cells to neural precursors. Promoters of these G9a-repressed genes were AT rich and H3K9me2 enriched but H3K4me3 depleted and were not highly DNA methylated. Representative genes were found to be close to the nuclear periphery, which was significantly enriched for G9a-dependent H3K9me2. Strikingly, although 73% of total genes were early replicating, more than 71% of G9a-repressed genes were late replicating, and a strong correlation was found between H3K9me2 and late replication. However, G9a loss did not significantly affect subnuclear position or replication timing of any non-pericentric regions of the genome, nor did it affect programmed changes in replication timing that accompany differentiation. We conclude that G9a is a gatekeeper for a specific set of genes localized within the late replicating nuclear periphery.**

histone methylation | nucleus | replication timing | transcription

Posttranslational modifications of chromatin are central to the regulation of many chromosomal functions and are intimately tied to transcriptional regulation (1). The histone methyltransferase (HMTase) G9a, in a complex with G9a-like protein (GLP), is responsible for methylation of lysine 9 of histone H3 (H3K9me), commonly associated with gene repression (2, 3). Although H3K9 can be mono-, di-, or trimethylated (-me1, -me2, -me3, respectively), G9a-knockout ESCs have significantly reduced levels of H3K9me2 (2, 4, 5). H3K9me2 and H3K9me3 create a platform for the binding of heterochromatin protein 1 (HP1), usually associated with transcriptional silencing but sometimes required for transcriptional activation (6). G9a also recruits DNA methyltransferases via its ankyrin domain and can promote and/or maintain DNA methylation at target sites independent of its HMTase activity (7–10). G9a is an essential gene for development; knockout mice die at day 8.5 (3). Although the precise lethal event during development of G9a-null mice is not known, G9a ESCs can differentiate in culture but fail to methylate the promoter DNA of a set of genes during differentiation; this failure may affect stable silencing of those promoters (9). Despite the importance of G9a to gene expression and development, the cohort of genes regulated by G9a has not been reported. Moreover, it is not clear whether G9a always functions as a repressor or whether, as occurs at some promoters occupied by HP1 (6), it also can function to activate certain genes.

In addition to localized effects at specific promoters, G9a has global effects on chromatin organization. G9a-null cells show a loss of DNA methylation at major satellite DNA and several classes of repetitive and transposable elements (7). In addition, blocks of G9a-dependent H3K9me2 (large, organized chromatin K9 modifications, LOCKs) have been identified in mouse ESCs that appear to overlap strongly with chromatin associated with the nuclear lamina (11, 12). Interestingly, we previously showed that H3K9me2, but not H3K9me1 or H3K9me3, is enriched in the nuclear periphery and that G9a-null ESCs are selectively depleted of the H3K9me2 localized at the periphery (13). Chromatin at the nuclear periphery also is replicated late during S-phase, and differentiation of ESCs leads to changes in the replication timing of large chromatin domains, accompanied by the movement of those domains toward or away from the nuclear periphery and the respective silencing or activation of genes within those domains (14). Together, these results suggested the possibility that G9a may help establish compartments of facultative heterochromatin at the nuclear periphery. Here, we have investigated this hypothesis using a conditional-knockout ESC line that allows acute effects of G9a loss to be evaluated within the first several cell cycles following G9a disruption. We find that G9a loss leads to depletion of H3K9me2 at the nuclear periphery and de-repression of a set of genes with H3K9me2-enriched promoters. No genes were down-regulated, indicating that G9a is not required for the activation of transcription in ESCs. An overlapping set of genes was de-repressed by G9a loss in neural precursor cells (NPCs) derived from these ESCs. Intriguingly, the majority of G9a-repressed genes were late replicating, but the loss of G9a had no detectable effect on the replication timing of these genes or on the changes in replication timing that took place during ESC differenation to NPCs. We conclude that G9a mediates dimethylation of H3K9 within late-replicating chromatin at the nuclear periphery and is required within this genomic context to silence a defined set of genes.

## Results

**Changes in Histone Methylation Following G9a Knockout.** Stable and irreversible genetic knockout often leads to compensatory genetic and epigenetic changes that can confuse interpretation of the resulting phenotypes (15). For example, Suv39h1,2-knockout cells lose H3K9me3 but also gain H3K27me3 in pericentric heterochromatin, where it is not seen in wild-type cells (4). This kind of adaptation can be largely circumvented through the use of a conditional-knockout, in which cellular responses to the acute loss of the gene product can be monitored. We have constructed a conditional knockout of G9a in mouse ESC line TT2 (Fig. 1). This cell line has a single copy of the G9a gene flanked by loxP recombination sites and expresses 4-hydroxytamoxifen (OHT)-inducible Cre fusion protein (16). Addition of OHT results in the rapid deletion of G9a (Fig. 1*B*), a partial reduction in total H3K9me1 and H3K9me3, and a substantial reduction in total

Author contributions: D.M.G. designed research; T.Y., K.P., J.L., and I.H. performed research; M.T. and Y.S. contributed new reagents/analytic tools; T.Y., K.P., T.R., J.L., and I.H. analyzed data; and D.M.G. wrote the paper.

The authors declare no conflict of interest.

This article is a PNAS Direct Submission.

Data deposition: The data reported in this paper have been deposited in the Gene Expression Omnibus (GEO) database, www.ncbi.nlm.nih.gov/geo (accession no. GSE18082).

[1]Present address: Chiba Cancer Center Research Institute, 666-2 Nitona, Chuo, Chiba 260-8717, Japan.

[2]To whom correspondence should be addressed. E-mail: gilbert@bio.fsu.edu.

This article contains supporting information online at www.pnas.org/cgi/content/full/0906142106/DCSupplemental.

CELL BIOLOGY

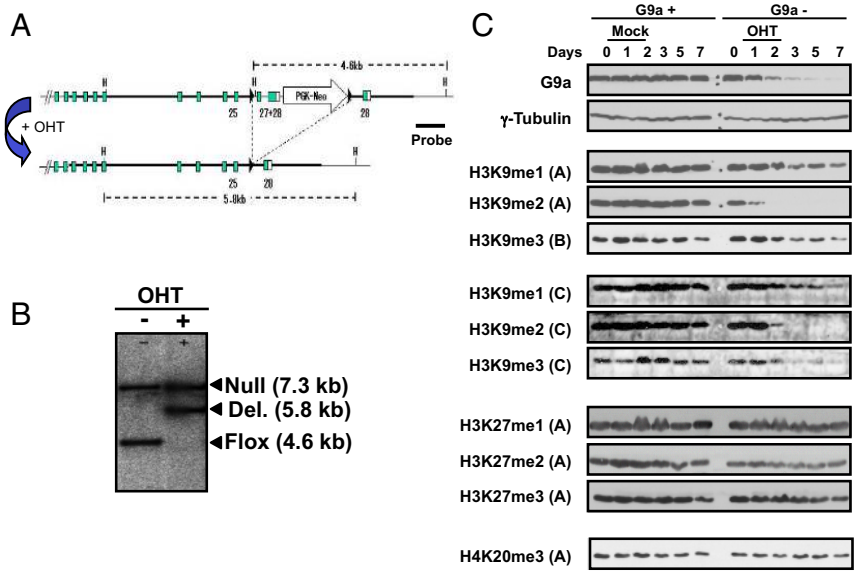


**Fig. 1.** Construction and characterization of a G9a conditional-knockout mouse ESC line. (*A*) When TT2G9a$^{flox/\Delta}$ ESCs are treated with OHT, the catalytic center of G9a is deleted, resulting in loss of a HindIII site that converts the 4.6-kb HindIII fragment on the floxed allele to a 5.8-kb HindIII fragment on the deleted allele. Also shown is the position of the probe used for Southern blot confirmation in (*B*). (*B*) Southern blot confirming genetic deletion of G9a 2 days after OHT treatment. The constitutively deleted allele produces a 7.3-kb fragment (3, 8). (*C*) Western blots of whole-cell extracts were performed at daily intervals after OHT or vehicle-only mock treatment and probed with antibodies against the indicated proteins or histone modifications. Histone antibodies are designated (A) for Upstate Biotechnology polyclonal antibodies, (B) for polyclonal anti-2xH3K9me3 antibodies (4), and (C) for monoclonal antibodies (17).

H3K9me2 (Fig. 1*C*), but has no effect on mono-, di- or trimethylated H3K27 or H4K20me3. The effects on the different methylated forms of H3K9 were similar with either commonly used polyclonal antibodies or more recently reported monoclonal antibodies (17) and were similar in a stable G9a-null ESC line. Hence, this conditional-knockout cell line provides the opportunity to observe the effects of acute G9a loss in the absence of complicating adaptive changes.

We previously reported that H3K9me2 is enriched at the nuclear periphery in human, mouse, and hamster fibroblasts, as well as in mouse ESCs, and that stable G9a-knockout ESCs preferentially lose peripheral H3K9me2 (13). To determine whether acute G9a loss also preferentially affects peripheral H3K9me2, we performed immunofluorescence detection of mono-, di- and trimethyl H3K9 before and after the addition of OHT (Fig. 2). H3K9me1 was distributed throughout the interior of the nucleus, excluding the periphery and clusters of pericentric heterochromatin (chromocenters), whereas H3K9me3 was localized primarily to the chromocenters; both these modifications show some reduction in signal after G9a loss but no change in localization. In contrast, H3K9me2

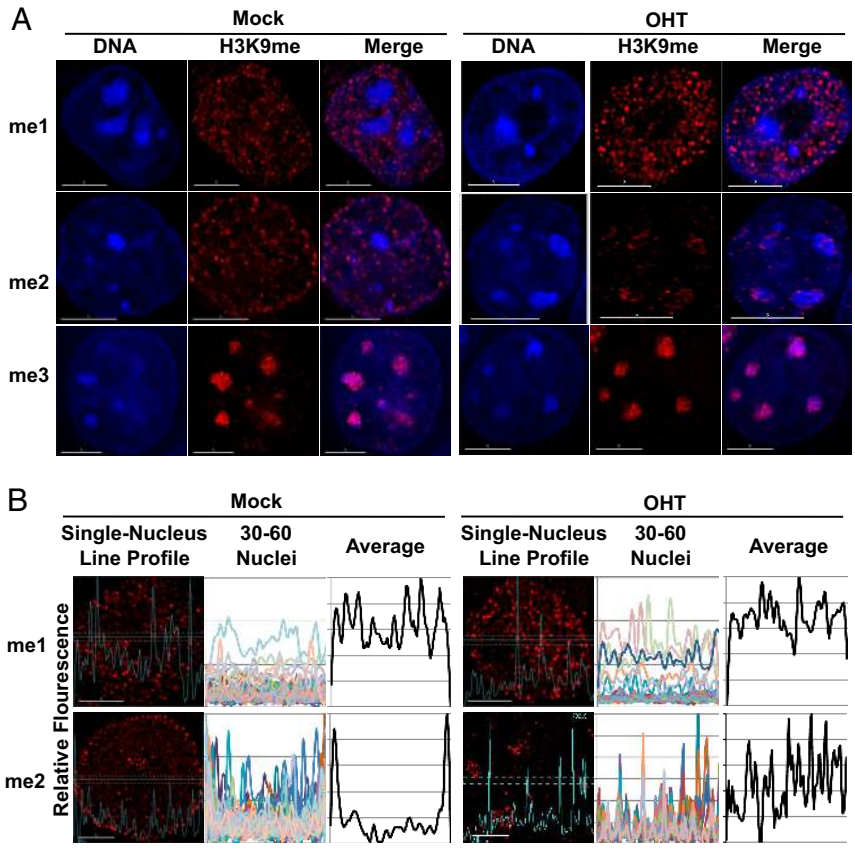


**Fig. 2.** G9a knockout leads to the selective loss of H3K9me2 at the nuclear periphery. (*A*) Cells were treated with OHT or were left untreated for 2 days, grown for an additional 5 days, and stained with monoclonal antibodies] against mono-, di- and trimethyl H3K9 (*red*). DNA was counterstained with DAPI (*blue*). (*B*) Quantification of H3K9me1 and H3K9me2 signal distribution for mock- and OHT-treated cells. (*Left*) Images show a single nucleus with a line 0.455 nm thick drawn through the diameter and a tracing of the density of immunofluorescence signal for each indicated antibody (me1 or me2). (*Middle*) Graphs are normalized line profiles from 30≈60 nuclei showing signal distribution across the nuclear diameter. (*Right*) Graphs are the average distributions from all nuclei across the nuclear diameter.

was most prominent at the periphery but also localized to some interior chromatin. G9a knockout led to complete loss of the peripheral signal and reduction of the internal signal but also a detectable increase at chromocenters. This increase also was detected in a stable G9a-knockout cell line (13). Hence, after G9a knockout, some H3K9me2 remains that is difficult to detect by Western blotting but is detected by immunolocalization, mostly at chromocenters. Taking these findings together, we conclude that G9a is the primary methyltransferase responsible for H3K9me2 at the nuclear periphery but that other mechanisms maintain low levels of this modification in other nuclear compartments.

**G9a Loss Leads to Up-Regulation of a Select Group of Genes.** To identify genes affected by G9a loss, we examined changes in transcript levels 7 days after OHT addition using microarray analysis. Comparison with mock-treated G9a$^{-/flox}$ cells identified 167 genes as more than 4-fold up-regulated and 10 genes as slightly more than 3-fold down-regulated (Fig. 3*A*). Analysis of a selection of the best-annotated (RefSeq) of these genes by RT-PCR verified 7/7 up-regulated genes, whereas down-regulated genes were affected less than 2-fold in the presence and absence of G9a (supporting information (SI) Fig. S1*A*). ChIP analysis revealed significant enrichment of H3K9me2 at the promoters of 7 up-regulated genes relative to an unaffected gene (Fig. 3*B*), consistent with these genes being targets of the G9a HMTase activity. Next, 4 days after the addition of OHT, we differentiated ESCs to NPCs for 9 days using a defined differentiation medium in adherent culture (18). These results revealed a set of 119 genes that were more than 4-fold up-regulated in OHT-treated vs. mock-treated cells (Fig. S1*B*), approximately one-third of which overlapped with the genes up-regulated in undifferentiated cells (Fig. 3*C*). Interestingly, genes up-regulated uniquely after differentiation to NPCs were developmentally regulated genes, mostly involved in vascular development and/or expected to be silent in NPC-derived lineages. A complete list of these genes and their properties can be found in Table S1. Inspection of results from a recent ChIP-chip analysis of H3K9me2 in mouse ESCs (11) revealed that the promoter regions of most up-regulated genes were significantly enriched for H3K9me2 (Fig. 3*D*), extending our individual gene results (Fig. 3*B*) and suggesting that the promoters of most of these genes are direct targets of the G9a HMTase activity. In fact, the set of genes that were found to be up-regulated in both ESCs and NPCs were significantly more enriched for H3K9me2 at their promoters than those up-regulated in either cell type alone (Table S1). Although we are not certain whether G9a represses all of these genes directly or indirectly, for the purposes of discussion we refer to them collectively as "G9a-repressed" genes.

Interestingly, G9a-repressed promoters are only a small subset of genes highly enriched for H3K9me2. Because the majority of H3K9me2 is lost after G9a deletion (Fig. 1), the repression of most of these H3K9me2-containing promoters must be maintained by other mechanisms. Most G9a-repressed genes do not fall within the previously identified LOCKs (11), but they are located within >50-kb regions of generally high H3K9me2 (Fig. S2) just below the threshold used to identify LOCKs. Although G9a-repressed genes were found on all chromosomes, they were highly enriched on the single X-chromosome in these male cells, particularly in differentiated cells (Fig. S3). The promoters of G9a-repressed genes also were unusually low in GC content (Fig. 3*E*), with 74.2% having low to intermediate CpG density (more than twice the fraction found in total genes as defined in ref. 19), mostly low in H3K4me3, and not enriched for either RNA pol II or DNA methylation relative to total genes. Interestingly, these genes are distinct from 126 genes whose promoters have high levels of G9a-dependent DNA methylation after retinoic acid-induced differentiation (9). Together these results identify a specific set of genes that are dependent upon G9a for their repression, many of which are H3K9 methylated but not highly DNA methylated despite the role of G9a in recruiting DNA methyltransferase.

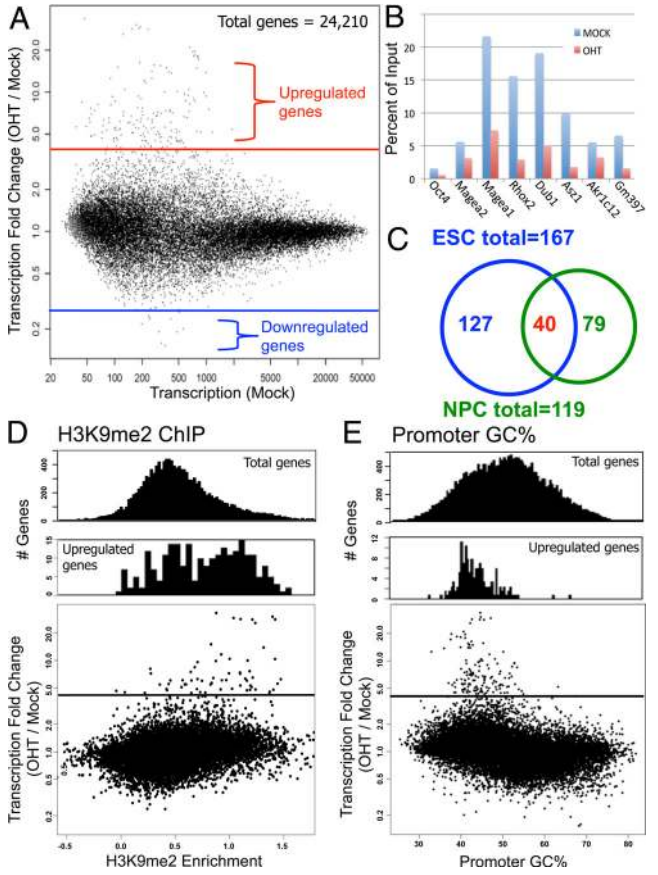


**Fig. 3.** Transcriptional changes after G9a knockout. (*A*) Following transcription microarray analysis, data normalization, and consolidation of probe values into 1 value per gene, gene expression values for all 24,210 genes identified on the NimbleGen microarray were plotted on the *x*-axis for mock-treated cells vs. the fold change for each gene after OHT treatment relative to mock treatment. A 4-fold increase in transcription was chosen as a cut-off (*red line*) for up-regulated genes; a 3-fold decrease in transcription was chosen as a cut-off (*blue line*) for down-regulated genes. (*B*) ChIP analysis for enrichment of H3K9me2 at the promoters of 8 genes that were either repressed (*Magea1*, *Magea2*, *Rhox2*, *Dub1*, *Asz1*, *Akr1c12*, *Gm397*) or unaffected (*Oct4*) by G9a knockout in ESCs. Immunoprecipitated DNA as well as DNA from the input was quantified by real-time PCR. (*C*) At 5 days after the addition of OHT, cells were differentiated to NPCs for 9 days. Microarray analysis was performed as in (*A*) (Fig. S1). Shown is a Venn diagram of the number of genes up-regulated after G9a deletion in ESCs (*blue*) and in NPCs (*green*) and those genes common to both ESCs and NPCs (*red*). (*D*) The total amount of H3K9me2 integrated over a region from 2 kb upstream to 0.5 kb downstream of the transcription start site of each gene was determined using previously published ChIP-chip data in mouse ESCs (11), and gene number was plotted as a function of H3K9me2 level. (*Top*) The number of total genes with each H3K9me2 value. (*Middle*) The number of up-regulated genes from (*A*) with each H3K9me2 value. (*Bottom*) The degree of up-regulation following G9a deletion vs. H3K9me2 for each gene. (*E*) (*Top*) The GC content surrounding each promoter ±1 kb from the transcription start site (total genes). (*Middle*) The GC content for the up-regulated promoter as in (*D*). (*Bottom*) A plot of the fold transcriptional change following G9a deletion vs. promoter GC%.

**Most G9a-Repressed Genes Are Induced Within Late-Replicating Chromatin.** Because the nuclear periphery is a late-replicating compartment (13), G9a-dependent enrichment of H3K9me2 at the nuclear periphery (Fig. 2) suggested that the HMTase activity of G9a is preferentially targeted to late-replicating chromatin. In fact, that H3K9me2 was strongly enriched within mid- to late-replicating chromosome domains (Fig. 4*A*). Furthermore, G9a-repressed

CELL BIOLOGY

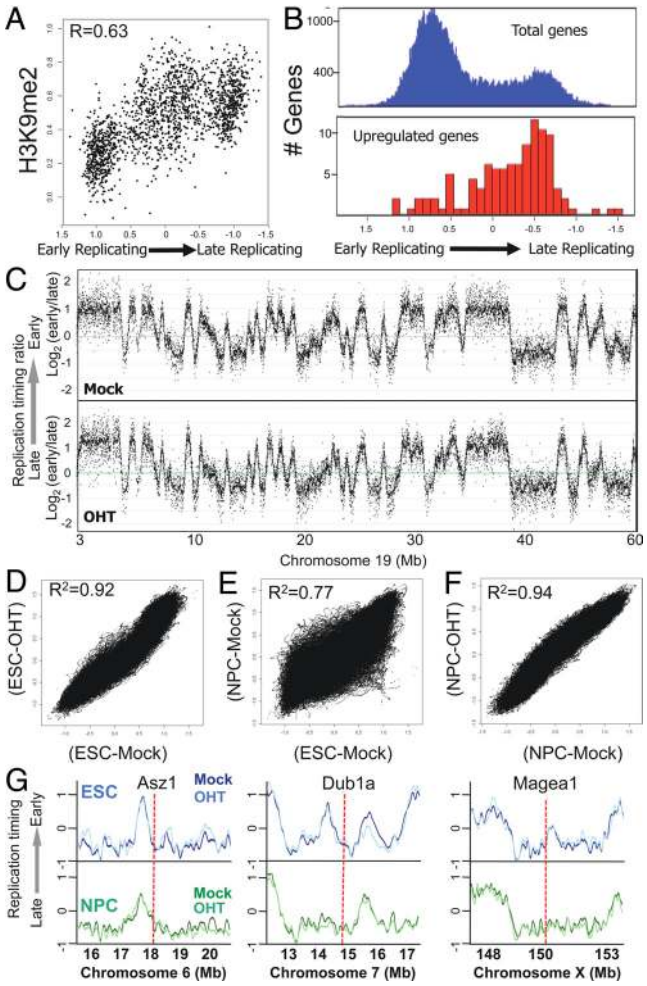


**Fig. 4.** Most G9a-repressed genes are late replicating. (*A*) The total amount of H3K9me2 integrated across each coordinately replicating chromosomal unit (replication domain, ref. 14) was plotted vs. the replication timing of each domain. Pearson's correlation coefficient is shown. (*B*) Histograms of the replication timing of total genes vs. G9a-repressed genes (*C*) An exemplary mouse ESC replication-timing profile of a chromosome 19 segment is shown for cells that were either mock or OHT treated. Averages of the raw values for probe log ratios [$Log_2$(Early/Late)] of 2 replicate samples (dye-swap) are plotted vs. the map position of each probe. (*D–F*) Scatter plots of probe values between the indicated conditions. (*G*) LOESS curves of replication timing in ESCs (*blue*) vs. NPCs (*green*) for either mock-treated (*darker shade*) or OHT-treated (*lighter shade*) cells. Shown are 5-Mb regions surrounding 3 highly up-regulated genes *Asz1*, *Dub1a*, and *Magea1*. The red dotted line indicates the map position of the gene.

genes are located within AT/long interspersed nuclear element-rich regions (LINE) (Table S1) that can switch replication timing during differentiation (14, 20). Finally, although ≈75% of genes are replicated in the first half of S-phase, nearly 75% of G9a-repressed genes were late replicating (Fig. 4*B*), and almost all genes up-regulated by more than 5-fold were late replicating (Table S1). Hence, G9a is the gatekeeper for the transcription of a set of late-replicating genes.

Because late replication is associated with gene silencing (21), these results raised the possibility that G9a may mediate late replication, potentially as part of the mechanism by which it represses these genes. To investigate the influence of G9a on replication timing, TT2 G9a$^{-/flox}$ cells were treated with or without OHT for 2 days, followed by 5 additional days of culture. Spectral karyotyping (SKY) was performed to verify genomic integrity after OHT treatment (Fig. S4). Replication timing was analyzed genome-wide using a previously described protocol (14). Briefly, cells were labeled with BrdU, sorted by flow cytometry into early- and late-S-phase populations, and BrdU-substituted DNA was immunoprecipitated, differentially labeled, and co-hybridized to a high-density whole-genome oligonucleotide microarray. This process generates a "replication-timing ratio" [$Log_2$(Early/Late)] for each of the tiled probes, which are positioned every 5.8 kb throughout the mouse genome. Replicates (dye-swap) showed high correlation [R = 0.74–0.83 for raw data and R = 0.95–0.96 for locally weighted scatter plot-smoothed (LOESS) data], and smoothed values were averaged. Fig. 4*C* shows a comparison of such averaged values for each probe across a 60-Mb segment of chromosome 19. Visual inspection of many such segments revealed no detectable changes in replication timing. Plotting all data points from mock- vs. OHT-treated cells relative to each other demonstrated a very high correlation between these data sets across the genome (Fig. 4*D*). We did detect an advance in the replication timing of major (but not minor) satellite DNA contained within the pericentric heterochromatin in G9a-knockout ESCs (22), consistent with a prior report (23). This finding could be related to the redistribution of H3K9me2 to pericentric heterochromatin (Fig. 2).

To investigate the possibility that G9a might play a role in replication timing changes that occur during differentiation, we differentiated TT2 G9a$^{-/flox}$ to NPCs using defined medium conditions (18) following mock- or OHT-treatment as in Fig. 3. Neural differentiation proceeded similarly with or without G9a, as verified by both transcription microarray and individual gene RT-PCR analyses. Replication timing was profiled genome wide after differentiation. As shown in Fig. 4*E*, differentiation elicited many changes in replication timing encompassing nearly 20% of the genome, consistent with previous results (14). However, comparison of mock- vs. OHT-treated NPCs showed high correlation (Fig. 4*F*), indicating that differentiation-induced changes in replication timing were unaffected by the loss of G9a. To determine whether localized changes in replication timing took place at G9a-repressed genes, LOESS tracings of the average replication timing values for 5-Mb regions surrounding 3 highly up-regulated genes were overlaid (Fig. 4*G*), revealing no detectable changes in replication timing as a result of G9a loss in either differentiated or undifferentiated cells. We conclude that G9a depletion leads to the induction of a class of late-replicating genes without affecting their replication timing or programmed changes in replication timing during differentiation. All replication timing and transcription microarray data are available for public viewing and downloading at ref. 24.

**G9a-Repressed Genes Localize to the Nuclear Periphery.** The above results demonstrate that H3K9me2 is enriched at the nuclear periphery and G9a is required to maintain H3K9me2 in the peripheral compartment (Fig. 2). Moreover, the nuclear periphery is a late-replicating (13) and generally repressive nuclear compartment (12, 25–27). These findings raised the question as to whether G9a-repressed genes are localized to the periphery. To address this question, we determined the subnuclear locations of 6 genes that were up-regulated in both ESCs and NPCs after G9a knockout by FISH and scored their radial distances from the periphery in mock- and OHT-treated ESCs relative to an unaffected gene. Results (Fig. 5) revealed that all 6 G9a-repressed genes were located near the nuclear periphery and remained near the periphery after G9a knockout, suggesting that G9a-repressed genes are enriched in the late-replicating peripheral compartment of the nucleus.

## Discussion

We demonstrate that the acute loss of HMTase G9a in mouse ESCs results in rapid depletion of H3K9me2 from the nuclear periphery and de-repression of 167 genes. G9a-deficient cells are capable of differentiation to NPCs, accompanied by the failure to repress a partially overlapping, set of 119 genes. Surprisingly, these genes are mostly late replicating, but their activation is not associated with a switch to early replication as usually is observed

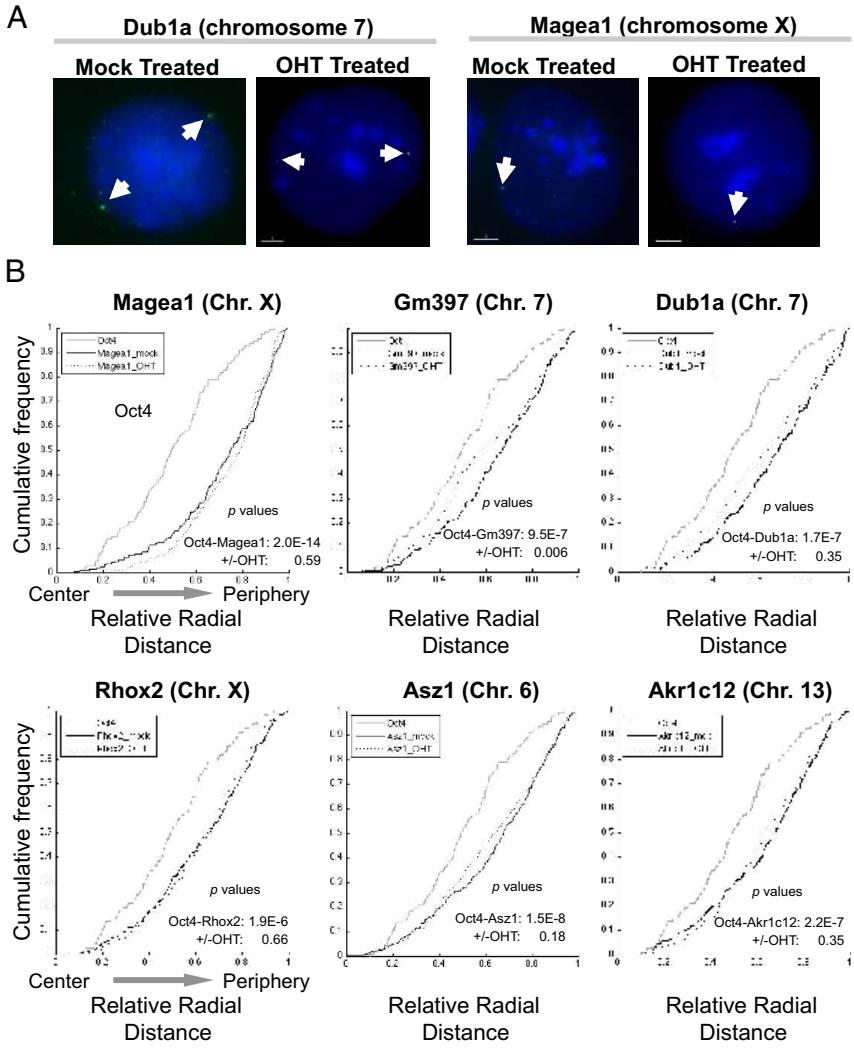


**Fig. 5.** G9a-repressed genes localize to the nuclear periphery. (*A*) FISH of mock- vs. OHT-treated cells using BAC probes for the indicated gene loci. DNA is counterstained in blue. White arrowheads point to the FISH signals (*green*). (*B*) At least 100 FISH signals for each experimental condition were scored, and the distance of each FISH signal to the nuclear periphery was normalized to the radius of the nucleus. Data are plotted as cumulative frequency graphs; the *x*-axis represents the relative radial distance to the nuclear periphery, where 0 represents the center and 1 the periphery of the nucleus.. Each graph shows 1 G9a-repressed gene (indicated above each graph) in mock-treated (*solid black line*) and OHT-treated (*dashed line*) cells, plotted alongside an internally localized gene (*Oct4*; *solid gray line*) that is unaffected by G9a knockout. *P*-values were calculated using a 2-sample Kolmogorov-Smirnov test.

for late-replicating genes that become activated during differentiation (14, 28, 29). In fact, almost complete depletion of H3K9me2 and partial depletion of H3K9me1 and H3K9me3 genome-wide resulting from G9a loss had no detectable effect on replication timing throughout the genome, except for a small effect on pericentric heterochromatin. We show that H3K9me2 is depleted selectively at the nuclear periphery upon G9a loss, and consistently we find G9a-repressed genes to be near the nuclear periphery. Our results demonstrate that, although G9a may act at many promoters and is known to affect the DNA and histone methylation of chromatin throughout the genome, it is directly responsible for the repression of a small set of late-replicating genes that are localized within peripheral heterochromatin.

Our results demonstrate that G9a is responsible for the majority of H3K9me2, as well as a fraction of H3K9me1 and H3K9me3, confirming and extending prior observations (2, 3, 5, 13). We also detect some remaining residual H3K9me2, including an increase in H3K9me2 in the pericentric heterochromatin, where G9a loss has been shown to cause a reduction in DNA methylation (7) and an increase in HP1-gamma (30). These changes in chromatin structure may account for a moderate karyotypic instability we observed following G9a loss and a slight advance in replication timing of major-satellite DNA (22, 23). The most dramatic qualitative effect of G9a loss is the selective loss of detectable H3K9me2 at the nuclear periphery (13).

Although some have reported results with specific genes derived from transcription microarray analysis of G9a-knockout mouse embryonic fibroblasts (30) or ESCs (31), we report the full set of genes affected by G9a. We find that, both in ESCs and after differentiation to NPCs, a surprisingly small number of genes are significantly de-repressed when G9a is lost. Most G9a-repressed genes harbor H3K9me2 at their promoters, suggesting that the repression by G9a is direct; however, few of these genes are DNA methylated. The lack of DNA methylation at G9a-repressed promoters may be related simply to the fact that many of them have a low CpG content and are poor substrates for DNA methyltransferase. However, G9a-repressed genes in NPCs did not overlap with genes whose promoter DNA methylation during retinoic acid-induced NPC differentiation was G9a dependent (9). Our differentiation system did not employ retinoic acid, but both differentiation systems enrich for NPCs, so these results suggest that many promoters that require G9a for DNA methylation during differentiation must be repressed by additional redundant mechanisms (e.g, the factors to express these genes may be missing). At these promoters, DNA methylation may be a fail-safe means to prevent their activation rather than the primary cause of their silent state (9).

Most interestingly, we find that the set of G9a-repressed genes is highly enriched in the late-replicating peripheral compartment of the nucleus that is selectively depleted of H3K9me2 after G9a loss. In fact, we find that H3K9me2, which has been shown to correlate with nuclear lamina-associated regions (11), is highly correlated

with late replication. Moreover, of the 126 previously identified genes with G9a-dependent promoter DNA methylation (9), more than 90% are early replicating, and at least 1 of these promoter-DNA-methylated genes (*Oct4*) is localized in the interior of the nucleus in both ESCs and NPCs (14). This finding suggests that the genes held in check by G9a are distinct from those whose promoters are DNA methylated as a result of G9a recruitment. Importantly, our results demonstrate that localization to the periphery of the nucleus is not sufficient to silence these genes. Not all late-replicating (14) or peripherally localized (25–27, 32) genes are silenced; strong, often CpG-rich, promoters can overcome the repressive effects of late replication (14). Hence, G9a loss and the depletion of H3K9me2 at the nuclear periphery may render these promoters strong enough to become easily accessible even within the context of a generally silent compartment. Our results also demonstrate that, consistent with observations in several other chromatin modifications (reviewed in ref. 21), replication timing is remarkably resilient to even dramatic changes in the amount of specific histone modifications.

## Methods

**Construction, Culture, and Differentiation of G9a$^{-/flox}$ ESCs.** Construction of conditional G9a$^{-/flox}$ ESCs from TT2 parental ESCs was described in figure S2 of ref. 33. ESCs were cultured as described (14). All experiments were set up as follows: $10^6$ cells were treated with 0.78 $\mu$M tamoxifen (4-OHT) or vehicle (ethanol) for 48 h and harvested 5 days later. SKY analysis was performed as a fee-for-service by the Roswell Park Cancer Institute SKY facility. Cells were differentiated 2 days after OHT or mock treatment, as described (18); the medium was changed every 2 days for 9 days.

**Immunofluorescence and Western Blots.** Immunofluorescence was performed as described (13, 34) using monoclonal antibodies specific for mono-, di-, or trimethylated H3K9 (17) and Alexa-Fluor 594-conjugated secondary antibodies (A-11032; Invitrogen/Molecular Probes). To quantify the signal distribution, line profiles were obtained for 30–60 randomly selected nuclei using the DeltaVision softWoRx program (Applied Precision). Lines of 0.455-nm width (7 pixels) were drawn through the diameter of the nuclei and normalized to the same relative length using LOESS regression analysis. Antibodies designated in Fig. 1 as (B) were gifts of T. Jenuwein (35); those designated (C) were gifts of H. Kimura (17). Other antibodies were obtained from Upstate Biotechnology for H3K9me1 (07–450), H3K9me2 (07–441), H3K9me3 (07–442), H3K27me1 (07–448), H3K27me2 (07–452), H3K27me3 (07–449), and H4K20me3 (07–749).

**Transcription and ChIP Microarray Analysis.** Total cellular RNA was isolated by RNeasy kit (Qiagen). Synthesis of cDNA and RT-PCR has been described (20). For microarray analysis, RNA specimens were converted to double-stranded cDNA, labeled with Cy3, and hybridized (Roche NimbleGen Systems) to use a mouse expression microarray representing 42,586 transcripts (NimbleGen 2006–08-03_MM8_60mer_expr). We identified 24,210 unique genes for further analysis. To determine the amount of H3K9me2 per promoter, published H3K9me2 values (11) were assigned to RefSeq gene positions based on the highest probe value from 2,000 bp upstream to 500 bp downstream of the promoter. Individual gene ChIP was performed using the ChIP-IT Enzymatic kit (Active Motif) following the manufacturers instructions, using an anti-H3K9me2 antibody (Abcam #1220). DNA was analyzed by real-time PCR.

**Replication Timing Analysis.** The replication profiling protocol has been described (14). It should be noted that, although mock- and OHT-treated cells were analyzed in parallel, replication timing data for mock-treated cells was previously reported (14), and Gene Expression Omnibus (GEO) submissions for these data sets are identical. Data analyses were performed using R/Bioconductor and Excel (Microsoft). Data normalization, calculation of the replication-timing ratio of 18,679 RefSeq genes [National Center for Biotechnology Information (NCBI)], identification of replication domains by segmentation, and calculation of GC and LINE-1 content of replication domains has been described (14). Segmentation was performed as described (14). Complete graphically displayed and downloadable replication-timing data sets for all 384,849 probes are available at ref. 24.

**Fluorescence in Situ Hybridization.** 2D FISH was performed as previously described (14), except that fixation was in 3:1 methanol:acetic acid, using digoxigenin-labeled commercially available bacterial artificial chromosome (BAC) probes prepared using the PrepEase BAC purification kit (USB #78722; USB Corporation). Images were collected with a DeltaVision imaging system. Measurements of the distance of FISH probes to the nuclear periphery and cumulative distance plots were made with the computer program FISH Finder (36).

**ACKNOWLEDGMENTS.** We thank S. Ty, J. Shirley, and X. Liu for development of the FISH Finder program used to analyze subnuclear position, H. Kimura and T. Jenuwein for supplying antibodies, X. Li for help with transcriptional analysis, R. Didier for flow cytometry, and S. Matsui for SKY analysis. This work was supported by National Institutes of Health Grant GM083337 to D.M.G. and The Leukemia and Lymphoma Society Special fellowship to T.Y.

1. Li B, Carey M, Workman JL (2007) The role of chromatin during transcription. *Cell* 128(4):707–719.
2. Tachibana M, et al. (2005) Histone methyltransferases G9a and GLP form heteromeric complexes and are both crucial for methylation of euchromatin at H3–K9. *Genes Dev* 19(7):815–826.
3. Tachibana M, et al. (2002) G9a histone methyltransferase plays a dominant role in euchromatic histone H3 lysine 9 methylation and is essential for early embryogenesis. *Genes Dev* 16(14):1779–1791.
4. Peters AH, et al. (2003) Partitioning and plasticity of repressive histone methylation states in mammalian chromatin. *Mol Cell* 12(6):1577–1589.
5. Rice JC, et al. (2003) Histone methyltransferases direct different degrees of methylation to define distinct chromatin domains. *Mol Cell* 12(6):1591–1598.
6. Hediger F, Gasser SM (2006) Heterochromatin protein 1: Don't judge the book by its cover! *Curr Opin Genet Dev* 16(2):143–150.
7. Dong KB, et al. (2008) DNA methylation in ES cells requires the lysine methyltransferase G9a but not its catalytic activity. *EMBO J* 27(20):2691–2701.
8. Tachibana M, Matsumura Y, Fukuda M, Kimura H, Shinkai Y (2008) G9a/GLP complexes independently mediate H3K9 and DNA methylation to silence transcription. *EMBO J* 27(20):2681–2690.
9. Epsztejn-Litman S, et al. (2008) De novo DNA methylation promoted by G9a prevents reprogramming of embryonically silenced genes. *Nature Structural and Molecular Biology* 15(11):1176–1183.
10. El Gazzar M, et al. (2008) G9a and HP1 couple histone and DNA methylation to TNFalpha transcription silencing during endotoxin tolerance. *J Biol Chem* 283(47):32198–32208.
11. Wen B, Wu H, Shinkai Y, Irizarry RA, Feinberg AP (2009) Large histone H3 lysine 9 dimethylated chromatin blocks distinguish differentiated from embryonic stem cells. *Nat Genet* 41(2):246–250.
12. Guelen L, et al. (2008) Domain organization of human chromosomes revealed by mapping of nuclear lamina interactions. *Nature* 453(7197):948–951.
13. Wu R, Terry AV, Singh PB, Gilbert DM (2005) Differential subnuclear localization and replication timing of histone H3 lysine 9 methylation states. *Mol Biol Cell* 16(6):2872–2881.
14. Hiratani I, et al. (2008) Global reorganization of replication domains during embryonic stem cell differentiation. *PLoS Biol* 6(10):e245.
15. Craig JM (2005) Heterochromatin—many flavours, common themes. *BioEssays* 27(1):17–28.
16. Sohal DS, et al. (2001) Temporally regulated and tissue-specific gene manipulations in the adult and embryonic heart using a tamoxifen-inducible Cre protein. *Circ Res* 89(1):20–25.
17. Kimura H, Hayashi-Takanaka Y, Goto Y, Takizawa N, Nozaki N (2008) The organization of histone H3 modifications as revealed by a panel of specific monoclonal antibodies. *Cell Struct Funct* 33(1):61–73.
18. Ying QL, Stavridis M, Griffiths D, Li M, Smith A (2003) Conversion of embryonic stem cells into neuroectodermal precursors in adherent monoculture. *Nat Biotechnol* 21(2):183–186.
19. Mohn F, et al. (2008) Lineage-specific polycomb targets and de novo DNA methylation define restriction and potential of neuronal progenitors. *Mol Cell* 30(6):755–766.
20. Hiratani I, Leskovar A, Gilbert DM (2004) Differentiation-induced replication-timing changes are restricted to AT-rich/long interspersed nuclear element (LINE)-rich isochores. *Proc Natl Acad Sci USA* 101(48):16861–16866.
21. Hiratani I, Takebayashi S, Lu J, Gilbert DM (2009) Replication timing and transcriptional control: Beyond cause and effect-part II. *Curr Opin Genet Dev* 19(2):142–149.
22. Wu R (2005) Epigenetic regulation of DNA replication timing in mammalian cells. PhD thesis (State University of New York Upstate Medical University, Syracuse, NY).
23. Jorgensen HF, et al. (2007) The impact of chromatin modifiers on the timing of locus replication in mouse embryonic stem cells. *Genome Biology* 8(8):R169.
24. Weddington N, et al. (2008) ReplicationDomain: A visualization tool and comparative database for genome-wide replication timing data. *BMC Bioinformatics* 9(1):530.
25. Kumaran RI, Spector DL (2008) A genetic locus targeted to the nuclear periphery in living cells maintains its transcriptional competence. *J Cell Biol* 180(1):51–65.
26. Reddy KL, Zullo JM, Bertolino E, Singh H (2008) Transcriptional repression mediated by repositioning of genes to the nuclear lamina. *Nature* 452(7184):243–247.
27. Finlan LE, et al. (2008) Recruitment to the nuclear periphery can alter expression of genes in human cells. *PLoS Genetics* 4(3):e1000039.
28. Hiratani I, Gilbert DM (2009) Replication timing as an epigenetic mark. *Epigenetics* 4(2):93–97.
29. Perry P, et al. (2004) A dynamic switch in the replication timing of key regulator genes in embryonic stem cells upon neural induction. *Cell Cycle*3(12):1645–1650.
30. Sampath SC, et al. (2007) Methylation of a histone mimic within the histone methyltransferase G9a regulates protein complex assembly. *Mol Cell* 27(4):596–608.
31. Kubicek S, et al. (2007) Reversal of H3K9me2 by a small-molecule inhibitor for the G9a histone methyltransferase. *Mol Cell* 25(3):473–481.
32. Luo L, et al. (2009) The nuclear periphery of embryonic stem cells is a transcriptionally permissive and repressive compartment. *J Cell Sci* 122(Pt 20):3729–3737.
33. Tachibana M, Nozaki M, Takeda N, Shinkai Y (2007) Functional dynamics of H3K9 methylation during meiotic prophase progression. *EMBO J* 26(14):3346–3359.
34. Wu R, Terry AV, Gilbert DM (2006) Observing S-phase dynamics of histone modifications with fluorescently labeled antibodies. *Methods in Molecular Biology* 325:139–148.
35. Perez-Burgos L, et al. (2004) Generation and characterization of methyl-lysine histone antibodies. *Methods in Enzymology* 376:234–254.
36. Ty S, Shirley J, Gilbert DM, Liu X (2009) Accurate boundary extraction and F.I.S.H. recognition in fluorescence images. Technical Report TR-090901 (Florida State University, Tallahassee, FL).